J Math Chem (2011) 49:2190–2209
DOI 10.1007/s10910-011-9880-x

ORIGINAL PAPER

Dynamics of benzene molecules situated in metal-organic frameworks

Yue Chan · James M. Hill

Received: 4 November 2010 / Accepted: 4 July 2011 / Published online: 16 July 2011

Abstract In this paper, we investigate the gyroscopic motion of a benzene molecule C_6H_6, which comprises an inner carbon ring and an outer hydrogen ring, and is suspended rigidly inside a metal-organic framework. The metal-organic framework provides a sterically unhindered environment and an electronic barrier for the benzene molecule. We model such gyroscopic motion from the inter-molecular interactions between the benzene ring and the metal-organic framework by both the Columbic force and the van der Waals force. We also capture additional molecular interactions, for example due to sterical compensations arising from the carboxylate ligands between the benzene molecule and the framework, by incorporating an extra empirical energy into the total molecular energy. To obtain a continuous approximation to the total energy of such a complicated atomic system, we assume that the atoms of the metal-organic framework can be smeared over the surface of a cylinder, while those for the benzene molecule are smeared over the contour line of the molecule. We then approximate the pairwise molecular energy between the molecules by performing line and surface integrals. We firstly investigate the freely suspended benzene molecule inside the framework and find that our theoretical results admit a two-fold flipping, with the possible maximum rotational frequency reaching the terahertz regime, and gigahertz frequencies at room temperature. We also show that the electrostatic interaction and the thermal energy dominate the gyroscopic motion of the benzene molecule, and we deduce that the extra energy term could possibly reduce the rotational frequency of the rigidly suspended benzene molecule from gigahertz to megahertz frequencies at room temperature, and even lower frequencies might be obtained when the strength of these interactions increases.

Y. Chan (✉) · J. M. Hill
Nanomechanics Group, School of Mathematical Sciences,
The University of Adelaide, Adelaide, SA 5005, Australia
e-mail: yue.chan@adelaide.edu.au

Keywords Benzene molecule · Metal-organic frameworks · Molecular gyroscope · Molecular turnstile · Sterically unhindered · Coulombforce · Lennard-Jones potential · Continuous approximation · Terahertz frequency

1 Introduction

Molecular rotors and molecular motors are widely occurring in nature. They range from powering the motion of internal molecular cells, such as adenosine triphosphate [1–3] to driving the whole body motion via a series of muscle contractions [4]. However, recent research places more emphasis on artificial molecular rotors and motors, such as molecular gears, carbon nanotube and fullerene based molecular oscillators, catenated porphyrin oscillatory systems, rope-skipping rotors and molecular turnstiles [5]. While the term molecular motor implies a discrete number of movable molecular components (molecular rotors) that perform mechanical-like movements in response to external stimuli, such as thermal heat, phonons [6], electrical fields [7,8,6] and fluidic flow [9]; the term molecular rotor refers specifically to those molecules that consist only of two components rotating relative to each other [5]. In addition, we can distinguish rotors from stators and rotators in that the latter are covalently bonded [5]. The vast majority of our current understanding of molecular rotors is dominated by synthesizing complex organic structures and examining their various properties embedded on a solid or in a solution [10,5,11,12]. A gigahertz linear motor comprising carbon nanotubes of various sizes has also been experimentally reported by Somada et al. [13]. From a medical point of view, molecular rotors have been used to measure micro-viscosity in liquids and living cells, from which the micro-viscosity has been shown to be directly linked to various diseases and the malfunction of cells [14–17]. Moreover, complex molecules which resemble macroscopic objects such as cars and wheelbarrows have been synthesized and can be controlled by a scanning tunneling microscope tip [18–21]. Such nanocars comprise C_{60} wheels and hydrocarbon chassis and the motion of the C_{60} wheels are actuated by thermally decoupling the C_{60} from the surface, so that they can rotate freely [22]. From all of these elaborate applications at the nanoscale, it is clear that a comprehensive understanding of the motion of nanoscale molecular motors is important.

Aromatic rings are found abundantly in all living organisms; for example in adenine, thymine, cytosine, guanine which form the bases of DNA. In addition, aromatic rings widely exist in numerous organic molecular systems such as benzene, pyridine and naphthalene. Knowledge of the minimum energy of aromatic rings becomes crucial to stabilize the global structure of proteins and DNA. In particular, benzene is an aromatic ring with the molecular formula C_6H_6 [23], which is formed from both natural processes and human activities. It is an important industrial solvent and a precursor in the production of drugs, resins, nylon, lubricants, pesticides, plastics, synthetic rubber, fibers and dyes. Isoreticular metal-organic framework structures (MOF), e.g. IRMOF-1 which is a cubic array of Zn_4O units bridged by benzenedicarboxylate (see Fig. 1) have been fabricated [24–28] and have been investigated for possible future applications, like gas storage [29–31], nonlinear optical properties [32] and industrial applications as a catalyst [33].

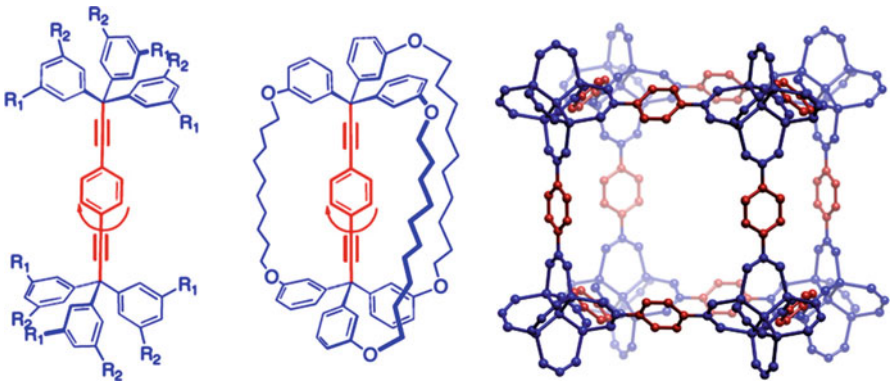

Fig. 1 Left and center: Structures that resemble macroscopic toy gyroscopes with open and triply bridged topologies; *Right*: a repeated unit of IRMOF-1, from which the 1,4-phenylenedicarboxylates is sterically unhindered but constitutes an electronic barrier (Copyright American Chemical Society 2008)

Metal organic frameworks are expected to form the basis of future molecular machinery design and the majority of molecular dynamics simulations investigate atomic and molecular diffusion and absorption inside the MOF [34–37]. Dynamics in guest-host materials has been a very active area of research, however only a few researches [38–40] examine molecular rotors inside a MOF, and in particular three-dimensional rotor arrays, i.e. benzene in MOF as a molecular gyroscope and a turnstile. The metal-organic framework structure carries rotators in a cubic cavity and provides rigid lattice points to support the aromatic ring, which is free to rotate, but is subject to the energetic penalty of rotating a carboxylic acid around a benzene unit, which might break the electronic conjugation with the carboxylates attached to the zinc atoms under the intrinsic rotational barrier. Although the chemical nature of the connecting bond, whether it is a single or a triple bond, is found to strongly influence the intrinsic barrier, there are discrepancies between the rotational barriers of such bonds as measured by experiments and those predicted by ab initio studies [41–43]. Unlike the triply bridged molecular gyroscopes, the 1,4-phenylene of the MOF is sterically unhindered, i.e. the molecules are not packed enough to slow down rotational motion but constitute an electronic barrier, that is an energy barrier due to the electrostatic force [44]. In this paper, we try to capture all these possible effects by incorporating a suitable empirical energy into the total molecular energy.

Guest-host structures often occur in chemical materials [5,38]. Experimental and computer simulation of such systems have been previously investigated by Devi et al. [38]. They propose benzene molecules as the stouts and IRMOF-105 rings as the host, and find that the benzene molecule rapidly moves around the C_6 axis over the entire temperature range, with an activation energy of 6 kJmol^{-1} by using ^{2}H NMR, and computational modeling confirms the molecular structure obtained from their experiments. Here, we investigate the gyroscopic motion of the rigidly suspended benzene molecule hopping inside the more complicated MOF system, i.e. IRMOF-105 (see Fig. 2). We first model the gyroscopic motion of a freely suspended aromatic ring by the inter-molecular interactions comprising the Coulomb force and the van der Waals force between the aromatic ring and the MOF, and we predict a two-fold

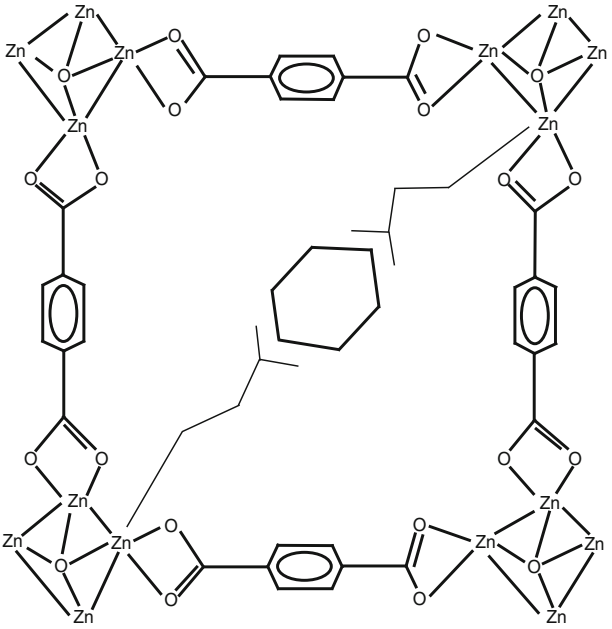

Fig. 2 Benzene molecule situated in MOF cross-section, where the molecule is non-covalently bonded with the MOF by ligands

flipping with the maximum rotational frequency reaching the terahertz range, which can be used to compare with experiments. Next, we incorporate an extra energy term into our model to take into account additional molecular interactions. We comment that although molecular dynamics simulations are widely employed for investigating such molecular dynamical problems, the methodology involves substantial computation to implement, and usually there are strict limitations on the spatial and time scales [45]. The continuous approximation presented here is computationally instantaneous through simply evaluating certain analytical integrations, and could easily be extended into more complicated molecular structures with little more computational time.

The paper is organized as follows: In section 2, we derive the theoretical background for the mechanics driving the gyroscopic motion of the benzene molecule inside the MOF, followed by numerical results and a discussion in section 3. Some conclusions are presented in the final section of the paper, and detailed mathematical evaluations are presented in three appendices.

2 Determination of total molecular energy using continuous approximation

Metal organic frameworks are sterically unhindered and provide an electronic barrier for a suspended benzene molecule [40,44,46], so that the dynamics of the benzene ring inside MOFs depends only on the intrinsic rotational barrier and the external thermal heat [46]. The intrinsic rotational barrier turns out to be part of the total

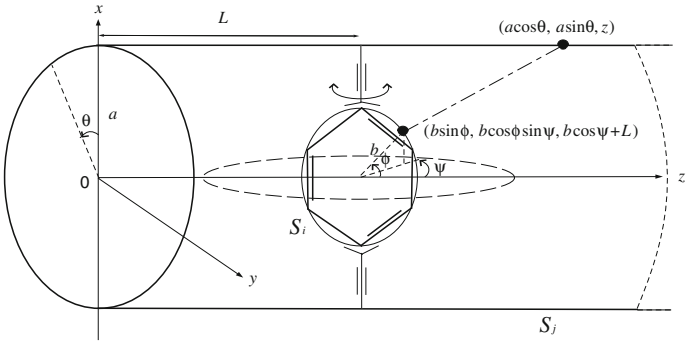

Fig. 3 Approximate model for benzene in MOF. Electrostatic energy is long range and semi-infinite cylinder accommodates such effects

molecular energy, while the external thermal heat perturbs the benzene molecule from its minimum molecular energy to induce a hopping motion. In addition, we assume that the benzene molecule is suspended non-covalently (or covalently bonded) but rigidly inside the MOF so that the motion of the benzene ring is driven by the electrostatic and van der Waals interactions between molecules in thermal equilibrium. We also incorporate an extra energy term into the total molecular energy to counteract certain additional molecular interactions, arising from sterical compensation of the carboxylate linkage.

Due to the periodic nature of MOFs, in order to make the problem mathematically tractable, we only consider one aromatic ring suspended rigidly at the center of the repeating unit of a MOF matrix but with an elongated extension to take into account the effect of the long-range electrostatic energy (see Fig. 3). In addition, we approximate the benzene molecule by two molecular rings, i.e. an inner carbon ring and an outer hydrogen ring, where the rings comprise six carbon atoms and six hydrogen atoms, respectively. In reality, all of the undulations in the potential energy governs the dynamics of the benzene molecule. However, for our approach, we consider an IRMOF-1 as the only MOF which has a cylindrically shaped cavity comprising 32 zinc atoms, 104 oxygen atoms, 96 carbon atoms and 48 hydrogen atoms as the nearest atoms. We further assume that all atoms are uniformly distributed over the surface of the two rings and the cylindrical cavity, so that the total molecular energy can be approximated by performing line and surface integrals. We model the inter-molecular energy as a combination of the Coulomb potential and the non-bonded 6–12 Lennard-Jones potential.

The total molecular energy of the gyroscopic system H_{tot} is therefore the sum of the electrostatic interactions between the carbon ring and the cavity $E_{(C-MOF)}$ and the hydrogen ring and the cavity $E_{(H-MOF)}$, the van der Waals interactions between the carbon ring and the cavity $V_{(C-MOF)}$ and the hydrogen ring and the cavity $V_{(H-MOF)}$, respectively, as well as an extra energy term U due to certain additional molecular interactions. Thus we have,

$$H_{tot} = E_{(C-MOF)} + E_{(H-MOF)} + V_{(C-MOF)} + V_{(H-MOF)} + U, \tag{1}$$

which we write symbolically as

$$H_{tot} = E + V + U, \tag{2}$$

where E and V denote $E_{(C-MOF)} + E_{(H-MOF)}$ and $V_{(C-MOF)} + V_{(H-MOF)}$, respectively, and we leave U as a suitable empirical form which will be determined later in the paper. We comment that we try to capture the gyroscopic motion of the benzene molecule as simply as possible to make the present mechanical model mathematically tractable without losing coarse details. In reality, for a MOF embedded in a liquid environment, hydrodynamic and Brownain forces, electrical double layer forces, solvation forces, hydrophobic forces, hydration forces, adhesion forces, frictional forces should also be considered [47]. For the Coulomb forces and van der Waals forces, within each ring-frame interaction, there are four separate ring-frame interactions $E_{(i-MOF,j)}$ and $V_{(i-MOF,j)}$, arising from the zinc, oxygen, carbon and hydrogen atoms, where i ($i = 1, 2$) and j ($j = 1, 2, 3, 4$) denote the type of the ring and the type of atoms on the MOF, respectively. Thus,

$$E_{(i-MOF)} = \sum_{j=1}^{4} E_{(i-MOF,j)} \qquad V_{(i-MOF)} = \sum_{j=1}^{4} V_{(i-MOF,j)}. \tag{3}$$

For $i = 1, 2$ and $j = 1, 2, 3, 4$, each van der Waals interaction $V_{(i-MOF,j)}$ can be determined according to Cox et al. [48,49], and can be approximated by

$$\begin{aligned} V_{(i-MOF,j)} &= \eta_i \eta_j \int\int \left\{ 4\epsilon_{ij} \left[\left(\frac{\sigma_{ij}}{\rho} \right)^{12} - \left(\frac{\sigma_{ij}}{\rho} \right)^{6} \right] \right\} dS_i dS_j \\ &= \eta_i \eta_j \int\int \left\{ -\frac{A_{ij}}{\rho^6} + \frac{B_{ij}}{\rho^{12}} \right\} dS_i dS_j = \eta_i \eta_j \left(-A_{ij} J_3 + B_{ij} J_6 \right), \end{aligned} \tag{4}$$

where η_i, η_j, ϵ_{ij}, σ_{ij}, ρ, S_i and S_j denote the atomic line density of the $i-$ring, the atomic surface density of j-atom on MOF, the potential well of i and j atoms, the distance at which the inter-particle potential of i and j atoms is zero, the inter-atomic distance, the line element of the rings and the surface element of the cavity, respectively. In addition, ϵ_{ij} and σ_{ij} are calculated using the Lorentz-Berthelot mixing rules [50] and using the values for the individual diatomic interactions. Likewise for each electrostatic energy $E_{(i-MOF,j)}$

$$E_{(i-MOF,j)} = \eta_i \eta_j \int\int \frac{q_i q_j}{\epsilon \rho} dS_i dS_j = \frac{\eta_1 \eta_2 q_i q_j}{\epsilon} J_{1/2}, \tag{5}$$

where q_i and q_j denote the residual charge for the i and j atoms, respectively. See Table 2 for a numerical value of ϵ and we comment that a MOF possesses a very high dielectric constant [51,52]. The value can range from as low as 60 to as high as 100 and we adopt the highest. For the lower value of ϵ, we find that the electronic rotational barrier increases and the hopping rate of the benzene molecule can only

Table 1 Lennard-Jones potential parameters. Note that LJ parameters for C are determined by [48,49], LJ parameters for H are determined by [57] and LJ parameters for atoms on MOF are determined by [31]

Benzene - MOF	Kinetic diameter σ_{ij} (Å)	Well depth ϵ_{ij} (eV)	Attractive constant A_{ij} (eVÅ^6)	Repulsive constant B_{ij} (eVÅ^{12})
C-Zn	2.931	0.00388	9.835	6235.658
C-C	3.416	0.00357	22.662	35977.420
C-O	3.259	0.00270	12.929	15490.660
C-H	2.986	0.00231	6.544	4633.570
H-Zn	2.930	0.00351	8.881	5613.295
H-C	3.172	0.00337	13.722	13970.960
H-O	3.094	0.00293	10.270	9000.773
H-H	2.957	0.00271	7.246	4841.504

reach the kilohertz frequencies. This might partially explain the ambiguity of current experimental values for the rotational barrier, from which we believe that the intrinsic electrical field strongly influences the gyroscopic motion. According to Fig. 3, the distance ρ between two typical points of the benzene molecule and the envisaged cylindrical surface of the MOF cavity can be written by

$$\begin{aligned}\rho^2 &= (a\cos\theta - b\sin\phi)^2 + (a\sin\theta - b\cos\phi\sin\psi)^2 + [(z-L) - b\cos\psi]^2 \\ &= a^2 - 2ab(\cos\theta\sin\phi + \sin\theta\cos\phi\sin\psi) + \\ &\quad b^2(1+\sin^2\phi\cos^2\psi) + (z-L)^2 - 2b(z-L)\cos\psi, \end{aligned} \tag{6}$$

where a and b denote the assumed average radii of the cylindrical cavity and the benzene molecule, respectively, and we also refer the reader to Table 2 for numerical values. In addition, the line and surface elements can be written by

$$dS_i = bd\phi, \qquad dS_j = ad\theta dz, \tag{7}$$

and given that we may perform the integrations in Eqs. (4) and (5), we may calculate the interaction energy. A detailed evaluation of J_n for $n = 1/2$, 3 and 6 is presented in Appendix A, from which, we can analytically determine the total molecular energy H_{tot} using Eq. (1).

3 Numerical result and discussion

In this section, we give numerical results for the theory outlined in section 2 using the parameters given in Tables 1 to 3. We first investigate the freely suspended benzene molecule situated inside a MOF by considering only the Columbic force and the van der Waals force as a first approximation. Then, as previously discussed we relax this approximation by incorporating an extra energy term U into the total molecular energy H_{tot} to take into account additional molecular interactions, for example arising from the sterical penalty induced by the carboxylate ligands between the benzene molecule

Table 2 Some parameters for benzene ring and metal-organic framework

Benzene molecule and MOF	Value
a	8.40 Å
b (Carbon ring)	1.40 Å
b (Hydrogen ring)	2.48 Å
m_C	12 m_u
m_H	1 m_u
ϵ	100ϵ_0

Table 3 Atomic surface density and the charge distribution [31]

Atom	Atomic density (no. atoms Å^{-2})	Charge
C (Benzene)	0.682	0.14e
H (Benzene)	0.385	0.12e
Zn	0.117	1.1e
C (Framework)	0.089	0.14e
O	0.036	−0.77e
H (Framework)	0.045	0.12e

and the MOF. A suitable empirical form for U is determined from the energy landscape predicted by the first approximation and from empirical energy forms in the literature [53].

3.1 Freely suspended benzene molecule situated in MOF

For the first approximation, with $U = 0$, we plot the total electrostatic energy E and the total Lennard-Jones potential energy V (see Eq. 1) in Figs. 4 and 5, respectively. Both numerical results feature two minimum potential (rotational) energies, which are located at $\psi = \pi/2$ and $\psi = 3\pi/2$ due to the π-symmetry of the benzene molecule, for which the surface of the benzene molecule is facing toward the envisaged open-end of the cavity. We also comment that these orientations have the largest total binding molecular interactions between the molecules. While the total electrostatic energy (see Fig. 4) has a potential well of 2 eV with a rotational barrier $W_E = W$ of 0.2 eV=4.6 kcal/mol, the total Lennard-Jones potential energy (see Fig. 5) has a much weaker potential well of −8.3 meV and a rotational barrier W_V of barely 3.2meV = 0.08 kcal/mol, due to the fact that the van der Waals force diminishes rapidly with distance [54]. We conclude that the gyroscopic motion of the freely suspended benzene molecule is driven mainly by the electrostatic interactions and the contribution from the Lennard-Jones potential can be largely ignored. These findings confirm the sterically unhindered nature of the MOF, that is the diminishing effect of the van der Waals force and the electrostatic force between the benzene molecule and the MOF provides an electronic barrier to the benzene molecule. We also comment that the small rotational barrier W, i.e. 4.6 kcal/mol and the binding energy, i.e. 2 eV are in good agreement with similar results reported by Devi et al. [38] but who only investigate a ring of

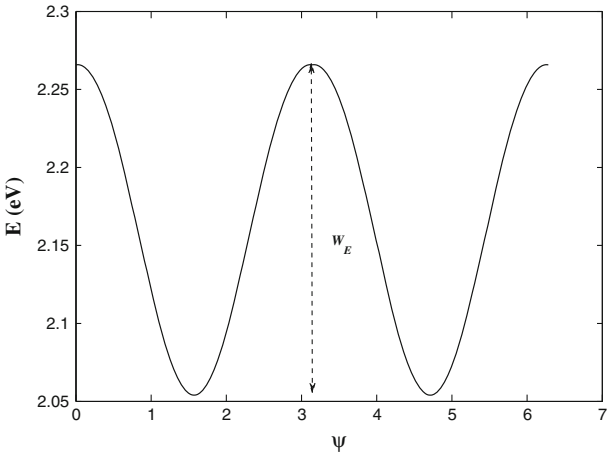

Fig. 4 Total electrostatic energy of the system

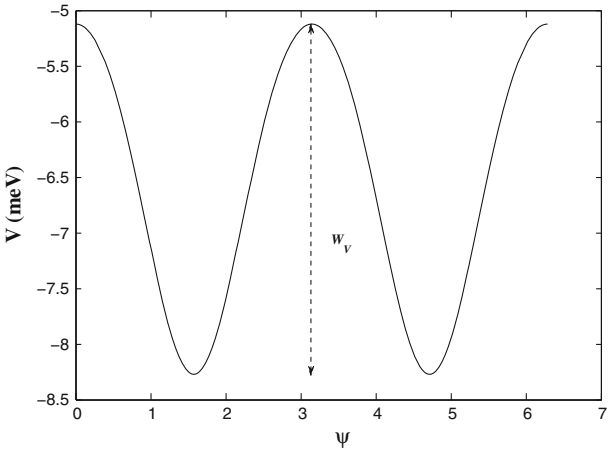

Fig. 5 Total van der Waals energy of the system

the MOF-105 structure, and for which the re-orientation of the molecular gyroscope occurs frequently at a sufficiently high temperature (see Fig. 6).

At absolute zero temperature, the benzene molecule is stationary in one of the two minimum total molecular energy configurations with equal probability, i.e. 50% chance. For a high temperature, i.e. $kT > W$, where k and T denote the Boltzmann's constant and the temperature, respectively, the rotational motion of the benzene molecule executes a classical Brownian motion. However, at a sufficiently low temperature, i.e. $kT < W$, the mechanism of the freely suspended benzene translates into a hopping motion, that is the benzene molecule will overcome the rotational barrier and flip between the two minimum energy states resulting in a rigid gyroscopic motion. Our theoretical study indicates an alternative explanation of the two-fold flipping, which is in agreement with the recent literature [40,46]. Upon assuming a small perturbation

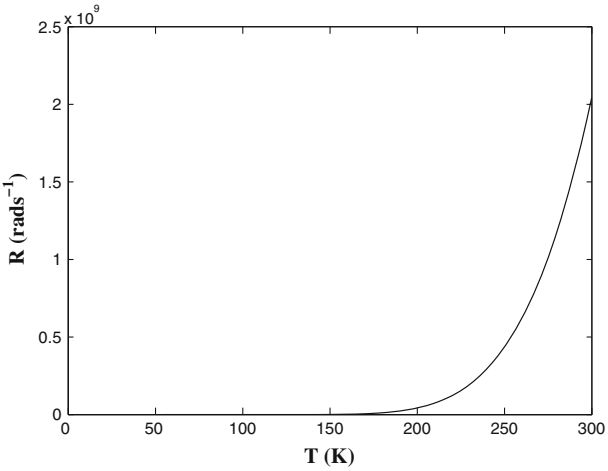

Fig. 6 Rate of thermally activated hopping

around the minimum potential energy, we can calculate the libration rotational frequency [55] or the maximum rotational frequency $\dot{\psi}$ of such system as

$$\dot{\psi} = (2W/I)^{1/2}, \tag{8}$$

where I denotes the moment of inertia of the benzene ring. Upon substituting W and I into Eq. (8), we obtain a value of the libration rotational frequency as 0.7 Tera Hz, which is in the terahertz range, and from which the rate of thermally activated hopping, R can be determined from the standard Boltzmann distribution [56], that is

$$R = \dot{\psi} exp(-W/kT). \tag{9}$$

The numerical result for R is plotted in Fig. 6, which clearly shows the notion of the thermal activation and predicts the gigahertz oscillation at room temperature, which is in good agreement with Devi et al. [38] that the hopping rate is not frozen even at 173K. We also believe that the assumption of no steric hindrance and low rotational barrier W for the MOF plays a significant role in generating the terahertz rotational frequency. The inter-molecular interaction and especially the electrostatic interaction is shown to be sufficient to generate the gyroscopic motion of the freely suspended bonded benzene ring inside the MOF, and which has not been fully exploited in the current literature [38,40,46,39]. We also comment that the major merit of our analytical approach is the very fast computational times using mathematical software packs, such as Maple, which rapidly evaluates special functions, such as the hypergeometric function.

3.2 Relaxation to first approximation

Next, we incorporate an extra energy term U arising from additional molecular interactions. We assume that sterical compensations contribute mainly to the torsional forces

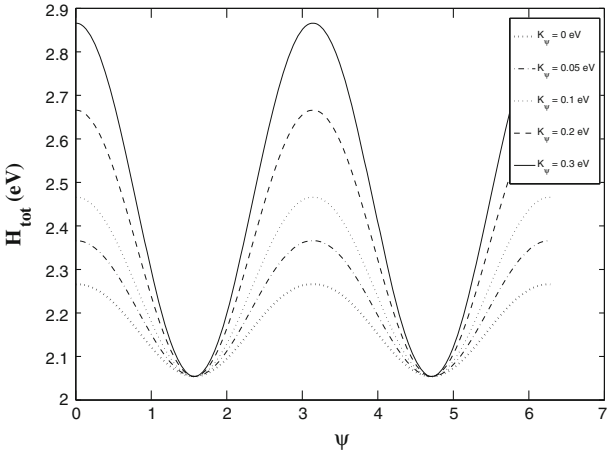

Fig. 7 Total molecular energies for $K_\psi = 0$ eV, 0.05 eV, 0.1 eV, 0.2 eV and 0.3 eV

which work against the rotational motion of the rigidly suspended benzene molecule. According to Tersoff [53] and the potential form derived in Appendix A for the freely suspended benzene molecule, we find that the most suitable empirical energy form satisfying all the basic requirements and being compatible with the current literature [53], is given by

$$U = \sum_{\psi} K_\psi \{1 + \cos(\eta\psi - \delta)\} = \sum_{\psi} K_\psi \{1 + \cos(2\psi)\}, \tag{10}$$

where K_ψ denotes the magnitude or strength of the additional molecular interactions. In addition, we choose $\eta = 2$ due to the two-fold flipping predicted from the first approximation, and we also assume that there is no phase difference between the rotation of the rigidly suspended benzene and the additional torsional forces arising from U, i.e. $\delta = 0$. We comment that since U depends only on ψ, the force generated by U is given by $-dU/d\psi$ which depends entirely on ψ leading to the retarding torsional forces acting on the rotating benzene molecule. We investigate four different values of K_ψ, namely 0.05 eV, 0.1 eV, 0.2 eV and 0.3 eV and the numerical results for the total molecular energies H_{tot} are shown in Fig. 7

We comment that for all the suggested values of K_ψ, the introduction of U preserves the general potential landscape of the gyroscopic system. In particular, the two fold flipping arises as a result of the potential form which is purposely chosen in Eq. (10). According to Fig. 7, we observe that an increase in the strength of K_ψ results in a higher rotational barrier W. The rotational barriers W for the prescribed values of K_ψ are given by 0.2, 0.3, 0.4, 0.6 and 0.8 eV which correspond to $K_\psi = 0$, 0.05, 0.1, 0.2 and 0.3 eV, respectively. Such increases in the rotational barriers caused by the introduction of U indicates that additional molecular interactions arising from some sterical penalties could generate higher rotation barriers for the rigidly suspended benzene molecule inside the MOF. Hence, the resulting rotational frequencies for the

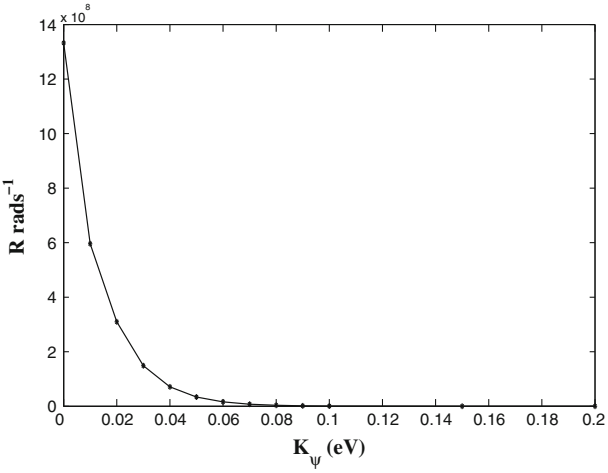

Fig. 8 Hopping rate R for various K_ψ at $T = 300$ K

benzene molecule are expected to decrease in comparison to the case of the freely suspended benzene molecule.

To verify this, we fix $T = 300$ K and employ Eq. (9) to evaluate the hopping rates of the rigidly suspended benzene molecule for different values of K_ψ ranging from 0 eV and 0.1 eV with an increment of 0.01 eV between each iteration, and the numerical results are shown in Fig. 8. According to Fig. 8, the hopping rate at room temperature decreases exponentially as the value of K_ψ increases. For example, the hopping rate at room temperature for $K_\psi = 0.1$ eV is given by 0.8M rads^{-1}, which is three order magnitude less than that for the freely suspended benzene molecule, i.e. 1.4G rads^{-1}. Similarly, we find that the hopping rate at room temperature for $K_\psi = 0.2$ eV reduces to 450 rads^{-1}. We conclude that the hopping rate is extremely sensitive to the strength of K_ψ so that the incorporation of U will certainly influence the gyroscopic motion of the rigidly suspended benzene molecule inside the MOF. This theoretical approach again provides very rapid results arising from the incorporation of U, which could otherwise take considerable computational time to implement using molecular dynamics simulations, and may provide an alterative elucidation to the discrepancies between various experimental and theoretical studies as discussed in the introduction.

4 Conclusion

Under the assumption of no steric hindrance and a small electronic barrier, we model the interaction of a rigidly suspended benzene molecule within a MOF, by including both the electrostatic force and the Lennard-Jones force. We also incorporate an extra energy term arising from additional molecular interactions into the total molecular energy to take into account certain sterical compensations. We approximate the benzene molecule by an inner ring of carbon atoms and an outer ring of hydrogen atoms, and also the MOF cavity by a cylindrical tube. The total molecular energy is determined by the continuous approach which assumes that a discrete atomic structure

can be approximated by average atomic densities over a line or a surface. We have purposely approximated the MOF cavity as an infinite cylindrical cavity because it represents the closest system to physical reality and adopting an infinite cylinder is an analytical device to evaluate the surface integrals. In reality, the short range Lennard-Jones interactions make no significant contribution since the long range electrostatic interactions dominates. We find that the gyroscopic motion of the freely suspended benzene molecule follows a two-fold flipping with the maximum rotational frequency reaching the teraherz range and gigahertz oscillation at room temperature, which can be used as a possible future high performance nano-rotor. Upon incorporating the extra energy term into the total molecular energy, we find that the general hopping rate drops dramatically owing to the fact that some sterical penalties might generate retarding torques, which work against the gyroscopic motion of the rigidly suspended benzene molecule. Further investigations will be to examine the covalently bonded benzene as a part of the MOF itself [39,40].

Acknowledgments We gratefully acknowledge the support from the Discovery Project Scheme of the Australian Research Council.

Appendix A: Analytical evaluation of integrals J_n

In this section, for convenience we carry out an analytical evaluation of $J_n(\psi)$ assuming that the tube length is infinite. The semi-infinite tube can be easily obtained as 1/2 that of the infinite tube. Given that, J_n can be written by

$$\begin{aligned} J_n = ab \int_{\theta=0}^{2\pi} \int_{z=-\infty}^{\infty} \int_{\phi=0}^{2\pi} & \frac{1}{\{a^2 - 2ab(\cos\theta \sin\phi + \sin\theta \cos\phi \sin\psi)} \\ & \frac{d\theta dz d\phi}{+b^2(1+\sin^2\phi\cos^2\psi) + (z-L)^2 - 2b(z-L)\cos\psi\}^n} \\ = ab \int_{\theta=0}^{2\pi} \int_{z=-\infty}^{\infty} \int_{\phi=0}^{2\pi} & \frac{d\theta dz d\phi}{(K_1 + K_2\cos\theta + K_3\sin\theta)^n}, \end{aligned} \tag{11}$$

where K_1, K_2 and K_3 denote $a^2 + b^2(1+\sin^2\phi\cos^2\psi) + (z-L)^2 - 2b(z-L)\cos\psi$, $-2ab\sin\phi$ and $-2ab\cos\phi\sin\psi$, respectively. Next, making use of $K_2 = K\cos\theta_0$ and $K_3 = K\sin\theta_0$, we can recast Eq. (11) into the following form

$$J_n = ab \int_{\theta=0}^{2\pi} \int_{z=-\infty}^{\infty} \int_{\phi=0}^{2\pi} \frac{d\theta dz d\phi}{\{K_1 + K\cos(\theta - \theta_0)\}^n}, \tag{12}$$

where $K = 2ab\sqrt{1-\cos^2\psi\cos^2\phi}$ and $\theta_0 = \arctan(\cot\phi\sin\psi)$. Upon making the substitution $\Theta = \theta - \theta_0$, taking into account the limits for an even function, and then using the half angle formula by defining $\theta = \Theta/2$, we obtain

$$J_n = 4ab \int_{\theta=0}^{\pi/2} \int_{z=-\infty}^{\infty} \int_{\phi=0}^{2\pi} \frac{d\theta dz d\phi}{\left\{(K_1 + K) - 2K \sin^2\theta\right\}^n}. \tag{13}$$

Eq. (13) can be integrated in terms of hypergeometric function which we then expand as a series to obtain

$$J_n = ab \sum_{k=0}^{\infty} \frac{(-1)^k 2^{k+1} \pi (n)_k (1/2)_k}{(1)_k k!} I_k, \tag{14}$$

where $(\cdot)_k$ denotes the Pochhammer symbol and I_k takes the form

$$\begin{aligned} I_k &= \int_{z=-\infty}^{\infty} \int_{\phi=0}^{2\pi} \frac{K^k}{(K_1 - K)^{n+k}} dz d\phi \\ &= \int_{\phi=0}^{2\pi} (2ab)^k (1 - \cos^2\psi \cos^2\phi)^{k/2} \times \\ &\quad \int_{z=-\infty}^{\infty} \frac{dz d\phi}{\left\{(z - L - b\cos\psi)^2 + (a - b\sqrt{1 - \cos^2\psi \cos^2\phi})^2\right\}^{n+k}}. \end{aligned} \tag{15}$$

Now, we substitute $z - L - b\cos\psi = (a - b\sqrt{1 - \cos^2\psi \cos^2\phi}) \tan\xi$ and Eq. (15) becomes

$$\begin{aligned} I_k &= \int_{\phi=0}^{2\pi} \frac{(2ab)^k (1 - \cos^2\psi \cos^2\phi)^{k/2}}{(a - b\sqrt{1 - \cos^2\psi \cos^2\phi})^{2n+2k-1}} d\phi \int_{\xi=-\pi/2}^{\pi/2} \cos^{2(n+k-1)}\xi d\xi \\ &= \frac{(2ab)^k \pi (2n + 2k - 3)!!}{(2n + 2k - 2)!!} g_k, \end{aligned} \tag{16}$$

where !! denotes the usual double factorial notation and g_k is defined by

$$g_k = \int_{\phi=0}^{2\pi} \frac{(1 - \cos^2\psi \cos^2\phi)^{k/2}}{(a - b\sqrt{1 - \cos^2\psi \cos^2\phi})^{2n+2k-1}} d\phi. \tag{17}$$

We note that Eq. (17) admits singularities when $a = b$ and $\psi = \pi/2$ or $3\pi/2$, which is essentially a consequence of the Pauli exclusion principle. Eq. (17) is still difficult to integrate analytically. After we recast the numerator into the same form as the denominator and introducing $\kappa = (1 - \cos^2\psi \cos^2\phi)^{1/2}$ and $\zeta = a - b\kappa$ so that

$\kappa = (a - \zeta)/b$ and adopting the binomial expansion for $(1 - \zeta/a)$ in the numerator leads to

$$g_k = \frac{1}{b^k} \sum_{i=0}^{k} (-1)^i C_i^k a^{k-i} h_{k,i}, \tag{18}$$

where $h_{k,i}$ denotes

$$h_{k,i} = \int_{\phi=0}^{2\pi} \frac{d\phi}{(a - b\sqrt{1 - \cos^2\psi \cos^2\phi})^{2n+2k-i-1}}. \tag{19}$$

We then multiply both numerator and denominator by $(a + b\sqrt{1 - \cos^2\psi \cos^2\phi})^{2n+2k-i-1}$ and upon performing the binomial expansion on the numerator, we obtain

$$h_{k,i} = \sum_{\ell=0}^{2n+2k-i-1} 4C_\ell^{2n+2k-i-1} a^\ell b^{2n+2k-i-\ell-1} p_{k,i,\ell} \quad , \tag{20}$$

where C_k^n are the usual binomial coefficients, and $p_{k,i,\ell}$ denotes

$$p_{k,i,\ell} = \int_{\phi=0}^{\pi/2} \frac{(1 - \alpha^2 \cos^2\phi)^{2n+2k-i-\ell-1}}{\left[a^2 - b^2(1 - \alpha^2 \cos^2\phi)\right]^{2n+2k-i-1}} d\phi, \tag{21}$$

where $\alpha = \cos\psi$. Now, we substitute $t = \cos^2\phi$ and Eq. (21) can be expressed in terms of Appell's hypergeometric function as follows,

$$\begin{aligned} p_{k,i,\ell} = {} & \frac{1}{2(a^2 - b^2)^{2n+2k-i-1}} \int_{t=0}^{1} \left\{ t^{-1/2}(1 - t)^{-1/2} \left(1 + \frac{b^2\alpha^2}{a^2 - b^2} t\right)^{-(2n+2k-i-1)} \right. \\ & \left. (1 - \alpha^2 t)^{2n+2k-i-\ell-1} \right\} dt, = \frac{\Gamma(1/2)^2}{2(a^2 - b^2)^{2n+2k-i-1}} \\ & \times F_1\left(\frac{1}{2}; 2n + 2k - i - 1, -2n - 2k + i + \ell + 1; 1; \frac{-b^2\alpha^2}{a^2 - b^2}, \alpha^2\right), \end{aligned} \tag{22}$$

where F_1 denotes the first Appell hypergeometric function. It is worthwhile noting that the Appell's hypergeometric function can be reduced to the usual hypergeometric function by a series sum, which can be handled easily by algebraic packages, such as Maple and Eq. (22) reads

$$p_{k,i,\ell} = \frac{\Gamma(1/2)^2}{2(a^2-b^2)^{2n+2k-i-1}} \sum_{m=0}^{\infty} \left\{ \frac{(-1)^m b^{2m} (1/2)_m (2n+2k-i-1)_m}{(1)_m m!(a^2-b^2)^m} \right.$$
$$\left. F(m+1/2, -2n-2k+i+\ell+1; m+1; \alpha^2) \right\} \alpha^{2m}. \tag{23}$$

Combining all the above results together, we obtain

$$J_n = \sum_{k=0}^{\infty} \sum_{i=0}^{k} \sum_{\ell=0}^{2n+2k-i-1} \sum_{m=0}^{\infty} \frac{(-1)^{k+i+m} \pi^2 a^{2k-i+\ell+1} b^{2n+2k-i-\ell+2m} (2n+2k-i-1)}{2^{2(n-2)}(n-1)!k!(k-i)!i!\ell!(2n+2k-i-\ell-1)!(m!)^2}$$
$$F(m+1/2, -2n-2k+i+\ell+1; m+1; \alpha^2)$$
$$\frac{\Gamma(k+1/2)\Gamma(m+1/2)(2n+2k-i+m-2)!\alpha^{2m}}{(a^2-b^2)^{2n+2k-i+m-1}} \tag{24}$$

We note that the singularity when b approaches a is preserved in Eq. (24) and we again comment that the semi-infinite solution can be obtained by simply multiplying Eq. (24) by the factor of 1/2.

Appendix B: Approximate solution for J_n

In this section, we assume $a \gg b$ and we derive an approximate expression for J_n (semi-infinite) and we find that such an approximations is not uniformly accurate in comparison with the full analytical solution derived in Appendix A. Starting from Eq. (19) we obtain

$$h_{k,i} = \frac{1}{a^{2n+2k-i-1}} \int_{\phi=0}^{2\pi} \left\{ 1 - (b/a)\sqrt{1-\alpha^2\cos^2\phi} \right\}^{-2n-2k+i+1} d\phi$$
$$\approx \frac{1}{a^{2n+2k-i-1}} \int_{\phi=0}^{2\pi} \left\{ 1 + \frac{b(2n+2k-i-1)}{a} \sqrt{1-\alpha^2\cos^2\phi} \right\} d\phi$$
$$= \frac{2\pi}{a^{2n+2k-i-1}} + \frac{4b(2n+2k-i-1)}{a^{2n+2k-i}} E(\alpha), \tag{25}$$

where $E(\alpha)$ denotes the complete elliptical integral of the second kind. Therefore, J_n can be approximated by

$$J_n = \sum_{k=0}^{\infty} \sum_{i=0}^{k} \frac{(-1)^{k+i} \pi^2 b}{2^{2(n-1)} a^{2(n-1)} \Gamma(1/2)(n-1)!k!(k-i)!i!}$$
$$\left\{ 2\pi + \frac{4b}{a}(2n+2k-i-1)E(\alpha) \right\} \tag{26}$$

For simplicity, we only give details for the van der Waals interaction and we note that the major difference between the approximate solution Eq. (26) and the full solution Eq. (24) is that the approximate solution excludes the effect of the singularity when b approaches a, which becomes significant for a large aromatic ring inside a condensed frame. Also, in comparison with the numerical results given by Fig. 5 and Fig. 9, although the approximate solution preserves the merit of two-fold flipping, we find that the approximate solution underestimates both the total van der Waals energy V and its intrinsic rotational barrier W_V. This is due to the fact that the ratio between the radius of the hydrogen ring and that of the MOF is not large enough for this approximation. The same conclusion can also be drawn for the total electrostatic energy. For purposes of benchmarking, we may increase the radius of the MOF and to find that

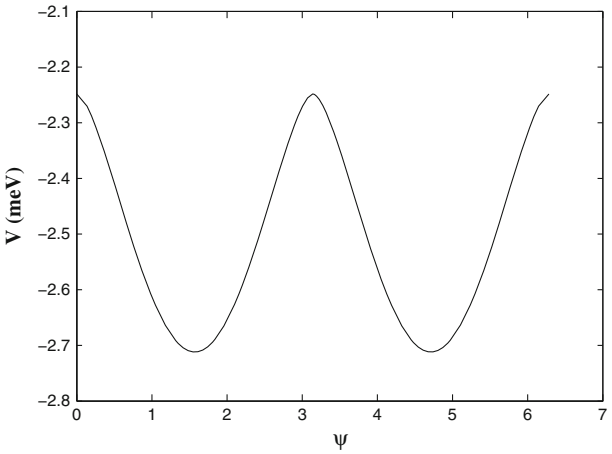

Fig. 9 Total approximate van der Waals energy of the system

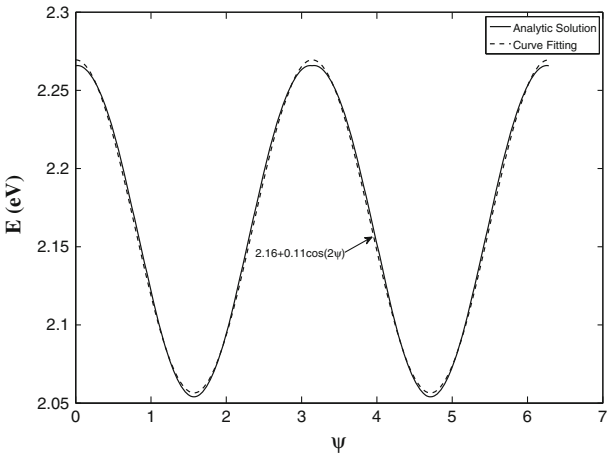

Fig. 10 Curve fitting for total electrostatic energy by two terms of Fourier cosine series

the full analytical solution approaches the approximate solution as the radius of the MOF increases.

Appendix C: Curve fitting

Since J_n possesses a periodic feature, it can be well approximated by a Fourier cosine series, which is convergent to the original function J_n. Due to the π-symmetry of the benzene molecule, the total electrostatic energy E can also be well approximated by the first terms of a Fourier cosine series, i.e. $a_0 + a_1 cos(2\psi)$, where a_0 and a_1 are constants, is plotted in Fig. 10 using the curve-fitting functionality in Matlab. We comment that while Eq. (24) looks complicated, it can be represented with increasing accuracy by the first few terms of the Fourier cosine series.

References

1. H. Itoh, A. Takahashi, K. Adachi, H. Noji, R. Yasuda, M. Yoshida, K. Kinosita, Mechanically driven ATP synthesis by F-1-ATPase. Nature **427**, 465–468 (2004)
2. P.D. Boyer, Molecular motors—what makes ATP synthase spin?. Nature **402**, 247 (1999)
3. R. Yasuda, H. Noji, K. Kinosita, M. Yoshida, F-1-ATPase is a highly efficient molecular motor that rotates with discrete 120 degrees steps. Cell **93**, 1117–1124 (1998)
4. M. Schliwa, G. Woehlke, Molecular motors. Nature **422**, 759–765 (2003)
5. G.S. Kottas, L.I. Clarke, D. Horinek, J. Michl, Artificial molecular rotors. Chem. Rev. **105**, 1281–1376 (2007)
6. J. Vacek, J. Michl, Artifical surface-mounted molecular rotors: Molecular dynamics simulations. Adv. Funct. Mater. **17**, 730–739 (2007)
7. D. Horinek, J. Michl, Molecular dynamics simulation of an electric field driven dipolar molecular rotor attached to a quartz glass surace. J. Am. Chem. Soc. **125**, 11900–11910 (2003)
8. D. Horinek, J. Michl, Surface-mounted altitudinal molecular rotors in alternating electric field: Single-molecular parametric oscillator molecular dynamics. Proc. Natl. Acad. Sci. USA **102**, 14175–14180 (2005)
9. J. Vacek, J. Michl, A molecular 'tinkertoy' construction kit: Computer simulation of molecular propellers. New J. Chem. **21**, 1259–1268 (1997)
10. E.R. Kay, D.A. Leigh, F. Zerbetto, Synthetic molecular motors and mechanical machines. Angew. Chem., Int. Ed. **46**, 72–191 (2007)
11. C.P. Mandl, B. Konig, Chemistry in motion-Unidirectional rotating molecular motors. Angew. Chem. Int. Ed. **43**, 1622–1624 (2004)
12. T.R. Kelly, Progress toward a rationally designed molecular motor. Acc. Chem. Res. **34**, 514–522 (2001)
13. H. Somada, K. Hirahara, S. Akita, Y. Nakayama, A molecular linear motor consisting of carbon nanotubes. Nano Lett. **9**, 62–65 (2009)
14. M.A. Haidekker, E.A. Theodorakis, Molecular rotors-Fluorescent biosensors for viscosity and flow. Org. Biomol. Chem. **5**, 1669–1678 (2007)
15. M.A. Haidekker, T. Brady, K. Wen, C. Okada, H.Y. Stevens, J.M. Snell, J.A. Frangos, E.A. Theodorakis, Phospholipid-bound molecular rotors: synthesis and characterization. Bioorg. Med. Chem. **10**, 3627–3636 (2002)
16. M.K. Kuimova, G. Yahioglu, J.A. Levitt, K. Suhling, Molecular rotor measures viscosity of live cells via fluorescence lifetime imaging. J. Am. Chem. Soc. **130**, 6672–6673 (2008)
17. M.A. Haidekker, T.P. Brady, S.H. Chalian, W. Akers, D. Lichlyter, E.A. Teodorakis, Molecular rotor derivatives-Synthesis and characterization. Bioorg. Chem. **32**, 274–289 (2004)
18. T. Sasaki, A.J. Osgood, L.B. Alemany, K.F. Kelly, J.M. Tour, Synthesis of a nanocar with an angled chassis. Toward Circling Movement. Org. Lett. **10**, 229–323 (2008)
19. T. Sasaki, J.M. Tour, Synthesis of a dipolar nanocar. Tetrahedron Lett. **48**, 5821–5824 (2007)

20. Y. Shirai, A.J. Osgood, Y.M. Zhao, Y.X. Yao, L. Saudan, H.B. Yang, Y.H. Chiu, L.B. Alemany, T. Sakaki, J.F. Morin, J.M. Guerrero, J.M. KellyK.F. Tour, Surface-rolling molecules. J. Am. Chem. Soc. **128**, 4854–4864 (2006)
21. F. Chiaravalloti, L. Gross, K.H. Rieder, S.M. Stojkovic, C. GourdonA. Joachim, F. Moresco, A rack-and-pinion device at the molecular scale. Nat. Mater. **6**, 30–33 (2007)
22. A.V. Akimov, A.V. Nemukhin, A.A. Moskovsky, A.B. Kolomeisky, J.M. Tour, Molecular dynamics of surface moving thermally driven nanocars. J. Chem. Theory Comput. **4**, 652–656 (2008)
23. J. Clayden, N. Greeves, S. Warren, P. Wothers, *Organic Chemistry* (Oxford University Press, Oxford, 2001)
24. S. Hermes, F. Schroder, R. Chelmowski, C. Woll, R.A. Fischer, Selective nucleation and growth of metal-organic open framework thin films on patterned COOH/CF3-terminated self-assembled monolayers on Au(111). J. Am. Chem. Soc. **127**, 13744–13745 (2005)
25. S. Hermes, D. Zacher, A. Baunemann, C. Woll, R.A. Fischer, Selective growth and MOCVD loading of small single crystals of MOF-5 at alumina and silica surfaces modified with organic self-assembled monolayers. Chem. Mater. **19**, 2168–2173 (2007)
26. E. Biemmi, C. Scherb, T. Bein, Oriented growth of the metal organic framework Cu-3(BTC)(2)(H2O)(3)·xH(2)O tunable with functionalized self-assembled monolayers. J. Am. Chem. Soc. **129**, 8054 (2007)
27. D. Zacher, A. Baunemann, S. Hermes, R.A. Fischer, Deposition of microcrystalline [Cu-3(btc)(2)] and [Zn-2(bdc)(2)(dabco)] at alumina and silica surfaces modified with patterned self assembled organic monolayers: Evidence of surface selective and oriented growth. J. Mater. Chem. **17**, 2785–2792 (2007)
28. Y. Yoo, Z. Lai, H.K. Jeong, Fabrication of MOF-5 membranes using microwave-induced rapid seeding and solvothermal secondary growth. Microporous Mesoporous Mater. **123**, 100–106 (2009)
29. N.L. Rosi, J. Eckert, M. Eddaoudi, D.T. Vodak, J. Kim, M. O'Keeffe, O.M. Yaghi, Hydrogen storage in microporous metal-organic frameworks. Science **300**, 1127–1129 (2003)
30. J.L.C. Rowsell, E.C. Spencer, J. Eckert, J.A.K. Howard, O.M. Yaghi, Gas adsorption sites in a large-pore metal-organic framework. Science **309**, 1350–1354 (2005)
31. R. Babarao, Z.Q. Hu, J.W. Jiang, S. Chempath, S.I. Sandler, Storage and separation of CO_2 and CH_4 in silicalite, C_{168} schwarzite, and IRMOF-1: A comparative study from monte carlo simulation. Langmuir **23**, 659–666 (2007)
32. S. Bordiga, C. Lamberti, G. Ricchiardi, L. Regli, F. Bonino, A. Damin, K.P. Lillerud, M. Bjorgen, A. Zecchina, Electronic and vibrational properties of a MOF-5 metal-organic framework: ZnO quantum dot behaviour. Chem. Commun. **20**, 2300–2301 (2004)
33. U. Mueller, M. Schubert, F. Teich, H. Puetter, K. Schierle-Arndt, J. Pastre, Metal-organic frameworks-prospective industrial applications. J. Mater. Chem. **16**, 626–636 (2006)
34. B.L. Huang, Z. Ni, A. Millward, A.J.H. McGaughey, C. Uher, M. Kaviany, O. Yaghi, Thermal conductivity of a metal-organic framework (MOF-5): PartII Measurement. Int. J. Heat Mass Transfer **50**, 405–411 (2007)
35. B. Civalleri, F. Napoli, Y. Noel, C. Roetti, R. Dovesi, Ab-initio prediction of materials properties with crystal: MOF-5 as a case study. Cryst. Eng. Comm. **8**, 364–371 (2006)
36. J.A. Greathouse, M.D. Allendorf, The interaction of water with MOF-5 simulated by molecular dynamics. J. Am. Chem. Soc. **128**, 13312–13312 (2006)
37. S. Amirjalayer, M. Tafipolsky, R. Schmid, Molecular dynamics simulation of benzene diffusion in MOF-5: Importance of lattice dynamics. Angew. Chem., Int. Ed. **46**, 463–466 (2007)
38. R.N. Devi, M. Edgar, J. Gonzalez, A.M.Z. Slawin, D.P. Tunstall, P.A. GrewalP. Cox, P.A. Wright, Structural studies and computer simulation of the inclusion of aromatic hydrocarbons in a zinc 2,6-naphthalene dicarboxylate framework compound. J. Phys. Chem. B **108**, 535–543 (2004)
39. E.B. Winston, P.J. Lowell, J. Vacek, J. Chocholousova, J. Michl, J.C. Price, Dipolar molecular rotors in the metal-organic framework crystalIRMOF-2. Phys. Chem. Chem. Phys. **10**, 5188–5191 (2008)
40. S.L. Gould, D. Tranchemontagne, O.M. Yaghi, M.A. Garcia-Garibay, Amphidynamic character of crystalline MOF-5: Rotational dynamics of Terephthalate Phenylenes in a free volume, sterically unhindered environment. J. Am. Chem. Soc. **130**, 3246–3247 (2008)
41. T. Kawaguchi, A. Mamada, Y. Hosokawa, F. Horii, H-2 nmr analysis of the phenylene motion in different poly(ethylene terephthalate) samples. Polymer **39**, 2725–2732 (1998)
42. A.L. Cholli, J.J. Dumais, A.K. Engel, L.W. Jelinski, Aromatic ring flips in a semicrystalline polymer. Macromolecules **17**, 2399–2404 (1984)

43. M. Tafipolsky, S. Amirjalayer, R. Schmid, Ab initio parametrized MM3 force field for the metal-organic framework MOF-5. J. Comput. Chem. **28**, 1169–1176 (2007)
44. T.A.V. Khuong, G. Zepeda, R. Ruiz, S.I. Khan, M.A. Garcia-Garibay, Molecular compasses and gyroscopes: Engineering molecular crystals with fast internal rotation. Cryst. Growth Des. **4**, 15–18 (2004)
45. N.M. Ghoniem, E.P. Busso, N. Kioussis, H. Huang, Multiscale modelling of nanomechanics and micromechanics: An overview. Philos. Mag. **83**, 3475–3528 (2003)
46. A.G. Miguel, E.G. Carlos, Engineering crystal packing and internal dynamics in molecular gyroscopes by refining their components Fast exchange of a Phenylene rotator by NMR. Cryst. Growth Des (2009)
47. Y. Liang, N. Hilal, P. Langston, V. Starov, Interaction forces between colloidal particles in liquid: Theory and experiment. Adv. Colloid Interface Sci. **134**(135), 151–166 (2007)
48. Cox B.J., Thamwattana N., Hill J.M. (2007) Mechanics of atoms and fullerenes in single-walled carbon nanotubes I Acceptance and suction energies. Proc. R. Soc. London, Ser. A 463:461
49. Cox B.J., Thamwattana N., Hill J.M. (2007) Mechanics of atoms and fullerenes in single-walled carbon nanotubesII Oscillatory behaviour. Proc. R. Soc. London, Ser. A 463:477
50. G.C. Maitland, M. Rigby, E.B. Smith, W.A. Wakeham, *forces-Their origin and determination* (Clarendon Press, Oxford, 1981)
51. D.W. Fu, H.Y. Ye, Q. Ye, K.J. Pan, R.G. Xiong, Ferroelectric metal-organic coordination polymer with a high dielectric constant. Dalton **7**, 874–877 (2007)
52. Q. Ye, Y.M. Song, G.X. Wang, K. Chen, D.W. Fu, P.W.H. Chan, S.D. ZhuJ.S. Huang, R.G. Xiong, Ferroelectric metal-organic framework with a high dielectric constant. J. Am. Chem. Soc. **128**, 6554–6555 (2006)
53. J. Tersoff, New empirical approach for the structure and energy of covalent systems. Phys. Rev. B **37**, 6991–7000 (1988)
54. J. Israelachvili, *Intermolecular and surface forces* (Academic Press, London, 1992)
55. H.A. Kramers, Brownian motion in a field of force and the diffusion model of chemical reactions. Physica **7**, 284 (1940)
56. R. Landauer, J.A. Swanson, Frequency factors in the thermally activated process. Phys. Rev. **121**, 1668–1674 (1961)
57. Maruyama S., Kimura T. *Molecular dynamics simulation of hydrogen storage in single-walled carbon nanotubes*. 2000 ASME International Mechanical Engineering Congress and Exhibit November 5–11:1–5, 2000